

Isotope effects between hydrogen and deuterium microwave plasmas on chemical vapor deposition homoepitaxial diamond growth

N. Mizuochi^{a)} and J. Isoya

Diamond Research Center, AIST, Tsukuba Central 2, Tsukuba, 305-8568, Japan; Graduate School of Library, Information and Media Studies, University of Tsukuba, Tsukuba, 305-8550, Japan; and CREST JST, Chiyoda Tokyo, 102-0081, Japan

J. Niitsuma and T. Sekiguchi

National Institute for Materials Science, Tsukuba, 305-0044, Japan

H. Watanabe, H. Kato, T. Makino, H. Okushi, and S. Yamasaki

Diamond Research Center, AIST, Tsukuba Central 2, Tsukuba, 305-8568, Japan and CREST JST, Chiyoda Tokyo, 102-0081, Japan

(Received 15 January 2007; accepted 6 March 2007; published online 16 May 2007)

This article shows that replacing hydrogen with deuterium improves the quality of microwave plasma-assisted chemical vapor deposition homoepitaxial diamond. Suppression of point defects in the bulk and of nonepitaxial crystallites and increasing of free-exciton emission intensity were revealed by electron paramagnetic resonance, optical microscopy, and cathodoluminescence, respectively. The isotope effects on the etching rate of diamond by deuterium are also revealed. The isotope effects are discussed from the viewpoint of etching effects. © 2007 American Institute of Physics. [DOI: 10.1063/1.2727380]

I. INTRODUCTION

Diamond has attracted significant interest as material for optical devices in the ultraviolet light emission regime and for high-power and high-frequency devices because of its superior physical and electrical properties.¹ Recently, high-quality diamond films with high Hall mobility²⁻⁴ and high growth rate⁵⁻⁷ are synthesized in microwave plasma-assisted chemical vapor deposition (MPCVD). Further improvements require the suppression of residual impurities and defects such as nonepitaxial crystallites (NC) and carbon dangling bond defects accompanying hydrogen atom (H1'), because these defects extensively influence diamond's electrical and optical properties.⁸⁻¹⁰

In CVD techniques, diamond is grown by hydrocarbon species predominantly composed of hydrogen (H₂). In plasma, electron impact with H₂ produces atomic hydrogen (H). It is well known that H plays important roles in the growth of high-quality diamond.¹¹ One of them is etching. It was previously reported that H selectively etches non-diamond-bonded material and graphite.¹¹ A theoretical study reports that H preferentially removes CH₂ moiety from the terrace of the (001) surface, promoting growth at steps (or kinks) and deposition of a smooth surface.¹² Promoting these effects is expected to improve quality.

Replacing H₂ with deuterium (D₂) reportedly increases the plasma etching rate in crystalline Si,¹³ reduces light-induced degradation in amorphous Si,¹⁴ and increases resistance of Si-D bond breaking above that of Si-H bonds at the Si surface and the Si/SiO₂ interface.¹⁵ MPCVD diamond films have been grown using D₂ to investigate the spatial distribution of D in the bulk of diamond¹⁶ or to assign vibra-

tional frequency of C-H bonds.¹⁷ However, isotope effects on MPCVD diamond growth have not been studied so these effects are the theme of this study.

II. EXPERIMENT

Diamond films were deposited epitaxially on high-pressure and high-temperature (HPHT) IIa and HPHT Ib single crystalline diamond (001) substrates with dimensions of 2.5 × 2.5 × 0.5 mm³ and 3.0 × 3.0 × 0.5 mm³, respectively (Sumitomo Electric Industries Ltd.). Their misorientation angles from (100) axis are shown in Table I. One benefit of a IIa substrate is that it prevents an overlap of strong electron paramagnetic resonance (EPR) signals of nitrogen. The films were grown in a MPCVD reactor using CH₄ (or CD₄) diluted with H₂ (or D₂) purified to more than 99.999 999 9% by a diffusion purifier (Japan Pionics Co. Ltd.). The substrate temperature was controlled by high-frequency heater independently of the input microwave (MW) power and kept at 1073 K as measured by a thermocouple attached to the back-side of a susceptor. The total gas pressure, total gas flow rate,

TABLE I. The growth conditions, NC densities, and C_{H1'}.

Film	Gas	Type	θ_{off}^a	Growth rate ^b	NC density	C _{H1'} /cm ³
D-I	CD ₄ /D ₂	IIa	4 ± 1°		<10 ³ /cm ²	(6 ± 3) × 10 ¹⁶
D-II	CD ₄ /D ₂	IIa	4 ± 1°		<10 ³ /cm ²	(2 ± 1) × 10 ¹⁷
D-III	CH ₄ /D ₂	IIa	4 ± 1°		<10 ³ /cm ²	(1 ± 0.5) × 10 ¹⁷
D-IV	CD ₄ /D ₂	Ib	<1°	0.12 μm/h	<10 ³ /cm ²	
D-V	CH ₄ /D ₂	Ib	<1°	0.13 μm/h	<10 ³ /cm ²	
H-VI	CH ₄ /H ₂	IIa	4 ± 1°		10 ⁴ –10 ⁵ /cm ²	(4 ± 2) × 10 ¹⁸
H-VII	CH ₄ /H ₂	IIa	4 ± 1°		10 ⁴ –10 ⁵ /cm ²	(4 ± 2) × 10 ¹⁸
H-VIII	CH ₄ /H ₂	Ib	<1°	0.27 μm/h	10 ⁴ –10 ⁵ /cm ²	

^a θ_{off} is misorientation angle from (001) axis.

^bThe experimental error of the estimation is less than 10%.

^aElectronic mail: mizuochi@slis.tsukuba.ac.jp

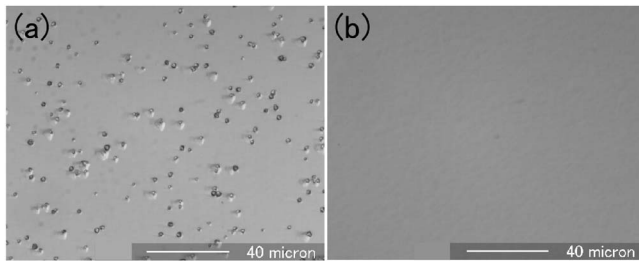


FIG. 1. The OM images of films grown by using (a) H_2 (H-VI) and (b) D_2 (D-V).

and input MW power were maintained constant at 25 Torr, 400 sccm, and 750 W, respectively. Deposition durations and $CH_4(CD_4)/H_2(D_2)$ ratios were 6 h and 0.5%, respectively. The thicknesses of films labeled D-IV, D-V, H-VIII were estimated by secondary ion mass spectroscopy (SIMS) or the step height between the substrate regions with and without a diamond mask. The thicknesses of films labeled D-I–III, H-VI–VII were simply estimated by deposition durations using the thickness data of films D-IV, D-V, H-VIII.

EPR spectra were measured by a Bruker ELEXSYS X-band spectrometer with a He cryostat. The CL measurements were performed at 200 K and acceleration voltages of 7 and 10 keV, which correspond to electron penetration depths of about 0.5 and 0.9 μm , respectively.¹⁸ The details of the EPR and CL measurements are described elsewhere.^{9,19} Optical emission spectra (OES) were obtained by using a charge-coupled device (CCD) detector. The emission light from the plasma was focused by a lens which is fixed to the MPCVD reactor. The focused light was transmitted by optical fiber with resolution of 2.1 nm to the CCD detector.

For estimation of etching rates, HPHT Ib single crystal-line (100) diamond was etched by inductively coupled plasma (ICP) (ULVAC Inc.). The power, bias voltage, pressure, and etching duration were 1 kW, 0 V, 4 Pa, and 4.5 h, respectively. As a mask of diamond etching, Au layers of 0.2 μm thickness were deposited by electron beam evaporation method. Au layers were removed by acid treatment after the etching. The etching rates were estimated by measuring a bump height between the Au covered surface and etched surface by stylus profiler (Dektak 8, Veeco Instruments).

III. RESULTS AND DISCUSSION

Using optical microscopy (OM) and EPR, we investigated NC and $H1'$ respectively, in films grown by CD_4/D_2 , CH_4/D_2 , and CH_4/H_2 . Figure 1 shows OM images of films. The NC densities are summarized in Table I, which shows that replacing H_2 with D_2 reduced the NC density by more than one order of magnitude.

The solid lines in Figs. 2(a) and 2(b) are EPR spectra of films grown by CH_4/H_2 (H-VI) and CD_4/D_2 (D-II), respectively. The g -values were estimated at 2.0026 ± 0.0001 . In H-VI, $H1'$ was clearly observed. An EPR line shape with a pair of partly resolved satellite lines with splitting of 1.25 mT, caused by the forbidden transitions of nearby H, is a characteristic of $H1'$ centers.¹⁹ In the previously reported films^{9,19} grown with the same condition of H-VI, the concentrations of $H1'$ ($C_{H1'}$) [$(3-8) \times 10^{18}/cm^3$] are almost the

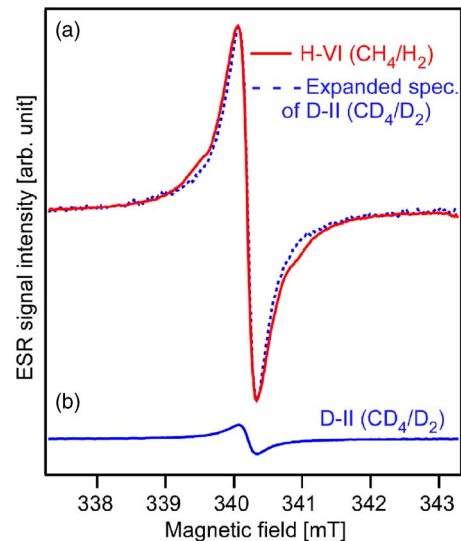


FIG. 2. (Color online) The EPR spectra in films (a) H-VI and (b) D-II at 40 K. The MW frequencies are 9.45 GHz. The MW power and the amplitude of 100 kHz field modulation were 0.1 mW and 0.07 mT, respectively. In (a), the signal intensity of film D-II (dotted line) is expanded to compare the EPR line shapes.

same as that of H-VI. It was clearly revealed that the defect concentration decreased more than 10 times by replacing H_2 with D_2 as shown in Fig. 2 and Table I.

In Fig. 2(a), the normalized spectrum of D-II grown by CD_4/D_2 is represented by a dotted line for comparison with the EPR line shapes. The g -value and the isotropic character of the spectra of D-I–III are identical to those of $H1'$. Figure 2(a) does not show the characteristic shoulder of $H1'$, which is reasonable where H is replaced with D. The splitting of the forbidden transition is approximately represented as $2(g_n \mu_n / g_e^2 \mu_B^2) h \nu$,¹⁹ where g_n and g_e are the nuclear and electronic g -values, respectively, μ_n and μ_B are corresponding Bohr magnetons, respectively, and h and ν are Planck's constant and MW resonant frequency of EPR, respectively. When H ($g_n=5.5857$) in $H1'$ is replaced by D ($g_n=0.8574$),²⁰ the splitting is calculated as about 0.2 mT, which can be hidden in the main peak. The SIMS measurement estimates the concentration of D in the film as $5-6(\pm 5) \times 10^{16}/cm^3$: almost identical to the spin concentration estimated from EPR. This suggests that the observed EPR signals in D-I–III mainly consists of that of $H1'$, where H is replaced with D, and that almost all H or D incorporated in our CVD diamond creates EPR active $H1'$ centers, whereas negative charged states of H-vacancy complex are observed in N -doped CVD diamond grown under high growth conditions.²¹

Figure 3(a) shows the CL spectra of films D-I and H-VI. The spectra are attributed to free-exciton emission associated with a transverse optical phonon (235 nm) and its replica (242 nm).²² Figure 3(b) shows the free-exciton signal intensities (I_{ex}) of D-I–III and H-VI–VIII at $\lambda=235$ nm, indicating that I_{ex} of D-I–III using D_2 is about 5 times larger than I_{ex} of H-VI–VIII using H_2 on average. Their ratios were almost the same between acceleration voltages of 7 and 10 keV.

The growth rates of films D-IV, D-V, H-VIII are shown

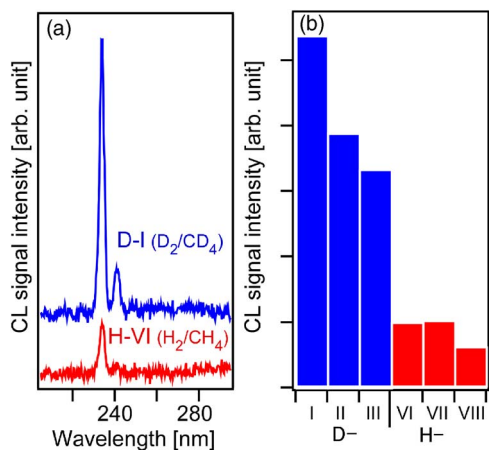


FIG. 3. (Color online) (a) The CL spectra of films D-I (upper) and H-VI (lower) at 100 K. The acceleration voltages of 10 keV. (b) The integrated signal intensity of free exciton of films D-I (CD_4/D_2), D-II (CD_4/D_2), D-III (CH_4/D_2), and H-VI (CH_4/H_2).

in Table I. The growth rate of H-VIII grown by CH_4/H_2 is typical for this synthesis condition.^{19,22} These results indicate that the growth rate using D_2 is almost half of that using H_2 . It was reported that $C_{\text{HI}'}$ decreases and I_{ex} increases as the growth rate decreases.^{1,9} In those results, when the growth rate is halved by the decrease of the CH_4/H_2 ratio, it can be extrapolated that $C_{\text{HI}'}$ decreases by half and about 80% of I_{ex} increases. If these quantities are subtracted from the total amounts of differences by replacing H_2 with D_2 , the substantial improvements by the isotope effects are estimated to be the decrease of one order of $C_{\text{HI}'}$ and the approximately 3 times increase of I_{ex} on average. Within our systematic experiments, this difference of CL intensity is beyond the experimental errors.

Diamond synthesis is always a competition between deposition and etching.^{11,12,23} The slower growth rate using D_2 can be assumed to be due to the higher etching effects of D compared with H as discussed in the following.

Isotope effects of electron- H_2 collision processes such as excitation and dissociation have been reported.^{24–26} One theoretical study focused on the isotope effects on the dissociation process of D_2 and H_2 through the ground state ($X^1\Sigma_g^+$) to the first excited state ($b^3\Sigma_u^+$) including vibrational levels.²⁴ Their calculations revealed a larger cross section of D_2 than that of H_2 , because the density of the states of the dissociation channel differs between H_2 and D_2 due to the energy difference of their vibrational levels. Through this process, the concentration of D in the plasma will probably be larger than that of H, which can promote the etching effect. We investigated the plasmas under our growth conditions by OES: a powerful technique for *in situ* diagnosis of plasma.²⁷ Figure 4 shows the OES spectra of H_2 and D_2 plasmas with the same growth condition parameters without methane. The compositions of gases in each plasma are (a) 100% H_2 ; (b) 50% H_2 and 50% D_2 ; (c) 100% D_2 ; and (d) 100% H_2 , respectively. They were measured consecutively from (a) to (d) only changing H_2 and D_2 without switching off the plasma. The Balmer lines labeled as H_α (D_α) at 656 nm and H_β (D_β) at 486 nm were observed. The wavelength differences of the Balmer lines between H and D are less than 0.2 nm,²⁸ which

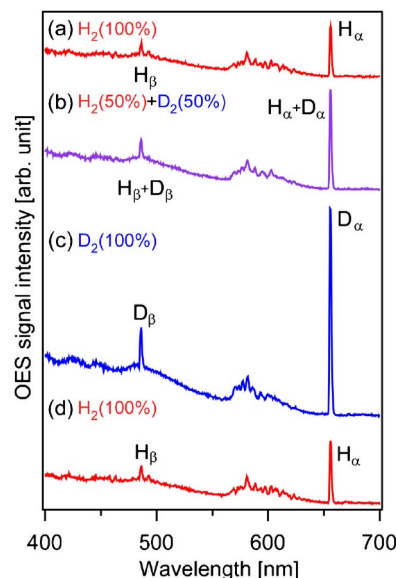


FIG. 4. (Color online) The OES spectra of H_2 and D_2 plasmas. The compositions of gases in each plasma are (a) 100% H_2 ; (b) 50% H_2 and 50% D_2 ; (c) 100% D_2 ; and (d) 100% H_2 , respectively. These spectra were measured consecutively from (a) to (d) by only changing the gases without switching off the plasma.

was less than our resolution of 2.1 nm. As Fig. 4 shows, the signal intensities significantly increased more than 4 times after H_2 was replaced by D_2 . Replacing D_2 by H_2 returned the signal intensities to (a). Because the emission processes of D_2 can be assumed to be the same as those of H_2 in the present condition, the increase of the signal intensity suggests a higher concentration of D than that of H.

Other studies have reported a larger cross section of the rotational excitation (τ_R) of D_2 than that of H_2 .^{22,23} Furthermore, τ_R of $J=0 \rightarrow 2$ is reportedly larger than τ_R of $J=1 \rightarrow 3$, where J is rotational quantum number. From nuclear statistics, the ratio of *ortho*- H_2 (*o*- H_2) to *para*- H_2 (*p*- H_2) is 3:1, while the ratio of *o*- D_2 to *p*- D_2 is 1:2. From the quantum-mechanical requirements, *o*- H_2 (D_2) can only exist in odd- J ($J=1, 3, \dots$) state and *p*- H_2 (D_2) can only exist in even- J ($J=0, 2, \dots$) state. Based on these effects, D_2 is expected to gain higher energy than H_2 in plasma, which can cause the energy of D to be higher than that with H. During syntheses, the substrate temperature was controlled by high-frequency heater equipment, which is independent of the microwave power sustaining plasma, and kept at 1073 K. In the syntheses by using D_2 , 15% decrease of the power of the high-frequency heating for substrate was observed. This presumably shows higher energy of D compared with H, which may further promote the etching effect.

It should be noted that a heat capacity (C_p) of D_2 at 298 K is 29.19 J/mol K which is the same with that of H_2 .^{29,30} Furthermore, C_p of atomic D is 20.8 J/mol K which is also the same as that of atomic H.^{29,30}

The thermal conductivities (k) of H_2 and D_2 at 300 K are $4.529 \times 10^{-4} \text{ cal cm}^{-1} \text{ s}^{-1} \text{ K}^{-1}$ and $3.405 \times 10^{-4} \text{ cal cm}^{-1} \text{ s}^{-1} \text{ K}^{-1}$, respectively.³¹ This indicates that the ability to transfer heat by H_2 is slightly higher than that of D_2 . On the other hand, it is indicated that larger heat is transferred to the sample in the D_2 synthesis compared with

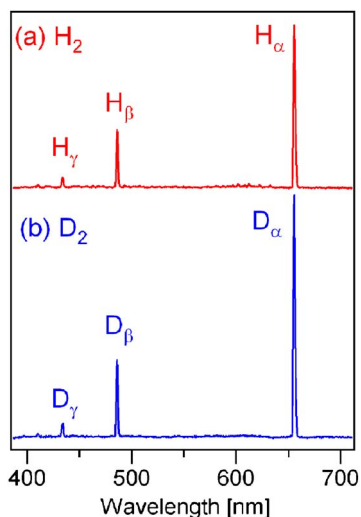


FIG. 5. (Color online) The OES spectra of (a) H_2 and (b) D_2 plasmas in the ICP.

that in the H_2 synthesis from the observation of the smaller power for the heating of the substrate. These may also support that the energy of molecules and atoms in the D_2 plasma is higher than those in the H_2 plasma. For the quantitative prediction of how much the difference of k contributes to the difference of the plasmas, further research is necessary.

Furthermore, we directly measured the etching rates of diamond by H_2 and D_2 in ICP etching. The OES spectra of the ICP are shown in Fig. 5. Similar to the spectra of Fig. 4, the emissions from H and D were observed. As seen from them, the signal intensity of D was about 30% stronger than that of H. Etching depths were measured as shown in Fig. 6. The bump heights by the etchings of H and D were estimated to be 400 and 480 nm, respectively. From them, the etching rates by H and D were estimated to be 89 and 107 nm/h, respectively. This indicates that the etching rate by D is about 20% larger than that by H in this condition.

Quantitatively, the etching rates in the MPCVD synthesis may be different from the ICP etching because of the difference of etching plasma conditions according to the difference of etching methods. In our conditions, the difference

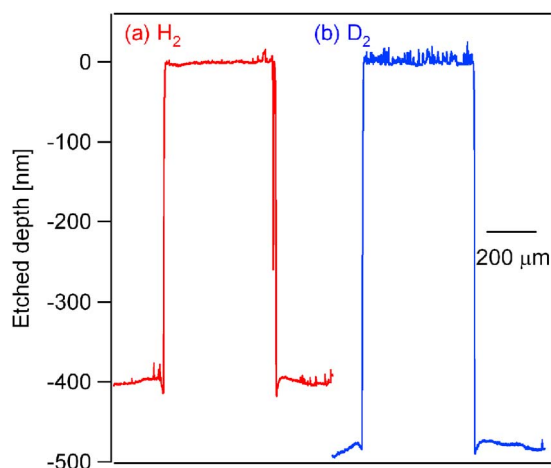


FIG. 6. (Color online) The etching depths by (a) H_2 and (b) D_2 . Each center region is the Au covered region.

of the OES signal intensity between H and D in the ICP etching was smaller than that of the MPCVD synthesis. It may be considered that the effects from the different dissociation processes with the calculated process through the ground state ($X^1\Sigma_g^+$) to the first excited state ($b^3\Sigma_u^+$) (Ref. 24) may be changed. If the etching rate can be assumed to be simply proportional to the relative OES signal intensity of H and D, the ratio of the etching rate by D to the etching rate by H in the MPCVD synthesis is considered to be larger than in the ICP etching.

As for the etching by D, it must have a different quality compared to the etching by H because the reduction in growth rate alone is apparently not sufficient to explain the data in this study. It can be supposed that the etching by D may promote the H etching effects for high-quality growth.^{11,12,23}

It should be noted that the difference of bond dissociation energies between H_2 and D_2 is small. Their values of H_2 and D_2 are 435.990 and 443.533 kJ/mol, respectively.³² Similarly, the differences of it between C-H and that of C-D are small, w 338.4 and 341.4 kJ/mol, respectively.³² It should be noted that, as for the isotope effect on increase of the resistance of Si-D bond breaking at Si surface and Si/SiO₂ interface, it is interpreted that the coupling of the Si-D bending mode to the Si bulk phonons results in an efficient channel for deexcitation.^{15,33} In diamond, as far as we know, such a correspondence of phonon frequencies is not reported. Therefore, the stability for C-D bond breaking at the surface can be considered to be almost the same as C-H in diamond.

IV. SUMMARY

The CVD homoepitaxial diamond films grown by D_2 plasma were investigated by OM, EPR, and CL, revealing suppression of the defect density and the increase of I_{ex} by replacing H_2 with D_2 . In the plasma of the present growth condition, higher concentration and higher energy of D compared with those of H are suggested, which can be considered to be the main sources of the isotope effect. From the ICP etching, the higher etching rate by D compared with that of H was demonstrated.

¹H. Okushi, *Diamond Relat. Mater.* **10**, 281 (2001).

²S. Yamanaka, H. Watanabe, S. Masai, D. Takeuchi, H. Okushi, and K. Kajimura, *Jpn. J. Appl. Phys., Part 2* **37**, L1129 (1998).

³H. Kato, H. Okushi, and S. Yamasaki, *Appl. Phys. Lett.* **86**, 222111 (2005).

⁴M. Katagiri, J. Isoya, S. Koizumi, and H. Kanda, *Appl. Phys. Lett.* **85**, 6365 (2004).

⁵J. Isberg, J. Hammersberg, E. Johansson, T. Wikström, D. J. Twitchen, A. J. Whitehead, S. E. Coe, and G. A. Scarsbrook, *Science* **297**, 1670 (2002).

⁶T. Teraji, K. Arima, H. Wada, and T. Ito, *J. Appl. Phys.* **96**, 5906 (2004).

⁷A. Tallaire, A. T. Collins, D. Charles, J. Achard, R. Sussmann, A. Gicquel, M. E. Newton, A. M. Edmonds, and R. J. Cruddace, *Diamond Relat. Mater.* **15**, 1700 (2006).

⁸D. Takeuchi, H. Watanabe, S. Yamanaka, H. Okushi, H. Sawada, H. Ichinose, and T. Sekiguchi, *Phys. Rev. B* **63**, 245328 (2001).

⁹N. Mizuochi, H. Watanabe, H. Okushi, S. Yamasaki, J. Niitsuma, and T. Sekiguchi, *Appl. Phys. Lett.* **88**, 091912 (2006).

¹⁰S. Yamanaka, H. Watanabe, S. Masai, S. Kawata, K. Hayashi, D. Takeuchi, H. Okushi, and K. Kajimura, *J. Appl. Phys.* **84**, 6095 (1998).

¹¹L. S. Plano, in *Diamond: Electronic Properties and Applications*, edited by L. S. Pan (Kluwer Academic, Dordrecht, 1995), Chap. 3, p. 64.

¹²C. C. Battaile, D. J. Srolovitz, I. I. Oleinik, D. G. Pettifor, A. P. Sutton, S.

- J. Harris, and J. E. Butler, J. Chem. Phys. **111**, 4291 (1999).
- ¹³H. Iwakuro, T. Kuroda, D. H. Shen, and Z. Lin, J. Vac. Sci. Technol. B **14**, 707 (1996).
- ¹⁴G. Ganguly, S. Yamasaki, and A. Matsuda, Philos. Mag. **63**, 281 (1991).
- ¹⁵J. W. Lyding, K. Hess, and I. C. Kizilyalli, Appl. Phys. Lett. **68**, 2526 (1996).
- ¹⁶J. Chevallier, F. Jomard, Z. Teukam, S. Koizumi, H. Kanda, Y. Sato, A. Deneuve, and M. Bernard, Diamond Relat. Mater. **11**, 1566 (2002).
- ¹⁷F. Fuchs, C. Wild, K. Schwarz, and P. Koidl, Diamond Relat. Mater. **4**, 652 (1995).
- ¹⁸K. Kanaya and S. Okayama, J. Phys. D **5**, 43 (1972).
- ¹⁹N. Mizuochi, H. Watanabe, J. Isoya, H. Okushi, and S. Yamasaki, Diamond Relat. Mater. **13**, 765 (2004); N. Mizuochi, M. Ogura, H. Watanabe, J. Isoya, H. Okushi, and S. Yamasaki, Diamond Relat. Mater. **13**, 2096 (2004).
- ²⁰J. A. Weil, J. R. Bolton, and J. E. Wertz, *Electron Paramagnetic Resonance* (Wiley, New York, 1994).
- ²¹C. Glover, M. E. Newton, P. M. Martineau, S. Quinn, and D. J. Twitchen, Phys. Rev. Lett. **92**, 135502 (2004).
- ²²H. Watanabe, K. Hayashi, D. Takeuchi, S. Yamanaka, H. Okushi, and K. Kajimura, Appl. Phys. Lett. **73**, 981 (1998).
- ²³S. G. Ri, H. Yoshida, S. Yamanaka, H. Watanabe, D. Takeuchi, and H. Okushi, J. Cryst. Growth **235**, 300 (2002).
- ²⁴C. S. Trevisan and J. Tennyson, Plasma Phys. Controlled Fusion **44**, 1263 (2002).
- ²⁵A. G. Engelhardt and A. V. Phelps, Phys. Rev. **131**, 2115 (1963).
- ²⁶H. Tawara, Y. Itikawa, H. Nishimura, and M. Yoshino, J. Phys. Chem. Ref. Data **19**, 617 (1990).
- ²⁷H. C. Barshilia and V. D. Vankar, J. Appl. Phys. **80**, 3694 (1996).
- ²⁸H. C. Urey, F. G. Brickwedde, and G. M. Murphy, Phys. Rev. **40**, 1 (1932).
- ²⁹M. Binnewies and E. Milke, *Thermochemical Data of Elements and Compounds* (Wiley, Weinheim, 2002).
- ³⁰Landolt-Börnstein, in *Thermodynamic Properties of Inorganic Materials, New Series, Group IV: Physical Chemistry*, edited by W. Martienssen (Springer, Berlin, 2000), Vol. 19.
- ³¹S. C. Saxena and V. K. Saxena, J. Phys. A **3**, 309 (1970).
- ³²J. A. Kerr and D. W. Stocker, in *CRC Handbook of Chemistry and Physics*, edited by D. R. Lide (CRC Press, Boca Raton, 2000).
- ³³C. G. van de Walle and W. B. Jackson, Appl. Phys. Lett. **69**, 2441 (1996).